# NOVEL COBALT SULFIDE-ETHYLENEDIAMINE NANOSHEETS FOR ADSORPTION-ASSISTED HEXAVALENT CHROMIUM REMOVAL*

Win Thi Yein[1], Qun Wang[2]

## Abstract

Hexavalent chromium, Cr (VI), contamination of wastewater is a great threat to living organisms and environment. Hence, the innovative advancement in the removal of Cr(VI) from wastewater is urgently on demand. The current research studied the influence of morphological and structural properties of CoS nanoadsorbents on the adsorption efficiency of Cr(VI) removal. The prepared CoS nanoadsorbents were synthesized with one-pot solvothermal/hydrothermal route without using toxic and harmful chemical reagents. The morphological and structural properties of prepared CoS nanoadsorbents were investigated by using various analytical techniques including Scanning Electron Microscopy (SEM), X- ray Diffraction (XRD) and FT-IR spectroscopy. The inorganic-organic hybrid CoS/En-nanoflowers gave the highest Cr(VI) removal efficiency from aqueous liquid compared to that of its counterparts such as CoS-nanorods and CoS-nanoflowers within 40 min. The Cr(VI) adsorption capacity of CoS/En-nanoflowers was found to be 87.7 mg/g and the adsorption process followed the pseudo-second-order kinetic model. Based on the theory of hard and soft acid-base (HSAB) and zeta potential results, the mechanism of Cr(VI) removal was suggested as electrostatic attraction between CoS/En surface and Cr(VI).

**Keywords:** inorganic-organic hybrid, nanosheets, adsorption, hexavalent chromium, electrostatic attraction

## Introduction

Hexavalent chromium, Cr (VI), pollution has become the most critical problem in recent years due to its high toxicity in human health and its persistence in the environment (Gupta et al., 2021). Various conventional methods including chemical precipitation, electrolysis, ion exchange, reverse osmosis, coagulation, and adsorption are being used as pollutants mitigation for the removal of Cr(VI). Among these, adsorption method is a low cost and high-efficiency technology to remove heavy metals. The conventional carbon adsorbents require high activation energy. The modified adsorbents either by crosslinking, grafting, changing the chemical form or through engineered composite materials have been put forward as a way to cost effective, and enhance the adsorption capacities (Manyangadze et al., 2020).

Compared to using conventional carbon adsorbents, inorganic-organic hybrid nanoadsorbents open up a new avenue towards the treatments of heavy metals contaminated wastewater. Recently, two-dimensional (2D) layered materials are gaining enormous interest as nanoadsorbent because of its high surface area and distinct layer structure (Wu et al., 2015). Non-layered cobalt sulfides possessing diverse chemical formulae ($Co_mS_n$) and various crystalline phases are difficult to design the atomically-thin 2D structure (Yein et al., 2018). Organic amine template-assisted fabrication is prominent to design nonlayered 2D atomically thin layer building blocks into 3D hierarchical structures through self-assembling growth process. There are researches on the fabrication of inorganic-organic metal sulfide-amines as alternative electrocatalysts for efficient energy conversion technologies (Liu et al., 2014; Ma et al., 2017). However, to our knowledge, the inorganic-organic hybrid CoS nanosheets used as a nanoadsorbent is rarely investigated to remove Cr(VI) from aqueous solution.

---

* Best Paper Award Winning Paper in Industrial Chemistry (2022)

[1] Department of Industrial Chemistry, University of Yangon

[2] School of Chemistry and Chemical Engineering, Harbin Institute of Technology, Harbin, China

Thus, the objectives of the present study are as follows: to fabricate CoS nanoadsorbents with different morphological and structural properties; to assess the adsorption efficiency of CoS nanoadsorbents on the Cr(VI) removal; and to gain deep insight into the adsorption mechanism of inorganic-organic hybrid CoS nanoadsorbent.

## Materials and Methods

### Materials

All the reagents used in this work were analytical grade without further purification. Cobalt acetate tetrahydrate ($Co(OAc)_2{\cdot}4H_2O$), thiourea ($SC(NH_2)_2$), ethylenediamine (En), potassium dichromate ($K_2Cr_2O_7$), hydrochloric acid (HCl) and sodium hydroxide (NaOH) were purchased from Shanghai Aladdin Bio-Chem Technology Co., Ltd. Deionized water was used as the solvent.

### Methods

### Preparation of CoS/En-nanoflowers

In a typical procedure, 0.10 mol of cobalt acetate tetrahydrate, and 0.15 mol of thiourea were dissolved into a volume ratio of ethylenediamine and water ($V_{En}$: $V_{H2O}$- 9:1) under vigorous stirring for 30 min. The solution was transferred into 20 mL Telfon-line stainless steel autoclave and heated at ~180˚C for 12 h. The resultant black product was collected and washed several times with distilled water and absolute ethanol. Finally, it was dried at ~70˚C for 12 h and ground to obtain the powder form. It was denoted as CoS/En-flowers.

### Preparation of CoS-nanoflowers

As a comparison, CoS-nanoflowers were synthesized in the identical procedure as mentioned above, with the same molar ratio of reagents and similar steps with the different volume ratio of ethylenediamine and water ($V_{En}$: $V_{H2O}$- 1:9) as solvent.

### Preparation of CoS-nanorods

As a comparison, CoS-nanorods were fabricated in the identical procedure as mentioned above, with the same molar ratio of reagents and similar steps with pure water ($V_{H2O}$-10) as solvent without adding ethylenediamine (En) as solvent.

### Characterization

The morphologies of the samples were examined by Hitachi field emission scanning electron microscope (FESEM, SU8100) at the accelerating voltage of 5.0 kV. The structure of the samples was determined by X-ray diffraction (XRD) on Rigaku D/max-2000 diffractometer. The functional groups in the samples were identified by using FT-IR spectroscopy (FT-IR-8400S, Shimadzu). Surface charges of samples were analyzed by a Zeta potential (Nano-ZS90 nanoparticle analyzer, Malvern Instruments Ltd.,).

### Batch Adsorption Experiments

Typically, 100 mg/L stock Cr(VI) solution was prepared by dissolving 0.1 g of potassium dichromate in 1.0 L of water (Vaddi et al., 2022). 100 mg of CoS samples were dispersed in 100 mL solution with a concentration of 100 mg/L of Cr(VI) solution and then the pH of Cr (VI) solution was adjusteds with 0.1 M HCl and 0.1M NaOH. The pH adjusted Cr(VI) solution was stirred in the dark for 120 min to reach the adsorption-desorption equilibrium. At a definite time interval, the suspensions were centrifuged, and the supernatant solution was taken to measure the

residual Cr(VI) concentration at 350 nm wavelength by using UV-Vis spectrophotometer (UV-1700, Shimadzu).

**Mathematical Equations**

The Cr(VI) removal efficiency of CoS samples was calculated by the following equation.

$$\text{Removal Efficiency (\%)} = \frac{C_o - C_e}{C_o} \times 100\ \% \qquad (1)$$

Where $C_0$ (mg/L) is the initial concentration of Cr(VI); $C_t$ (mg/L) and $C_e$ (mg/L) is the concentration of Cr(VI) ions at time *t* and equilibrium *e*. Kinetic models named pseudo-first-order and pseudo-second-order models were simulated for Cr(VI) adsorption on the adsorbent surface.

$$\log(q_e - q_t) = \log q_e - \frac{k_1 t}{2.303} \qquad \text{(Pseudo – first – order)} \qquad (2)$$

$$\frac{t}{q_t} = \frac{1}{k_2 q_e^2}\ \frac{t}{q_t} \qquad \text{(Pseudo – second – order)} \qquad (3)$$

Where $q_e$ and $q_t$ are the adsorbent absorption capacity (mg $g^{-1}$) at equilibrium and time. Moreover, $k_1$ and $k_2$ are the reaction rate constants ($min^{-1}$ and g $mg^{-1}$ $min^{-1}$) for the pseudo-first-order and pseudo-second-order, respectively.

## Results and Discussion

In the present study, the influence of solvent compositions on the morphological and structural properties of CoS samples were identified by serial microscopic and spectroscopic techniques. Firstly, the morphologies of CoS samples were examined by using SEM technique. Interestingly, when pure water was used as solvent medium, the morphology of the product was composed of nanorods as shown in Figure 1(a). In contrast, the volume ratio of En to water (1:9) under the identical conditions produced highly interconnected nanosheets assembled to form peony-flower-like structure CoS, named as CoS-nanoflowers as shown in Figure 1(b and c). The results indicated that the combination of a trace amount of En changed the sheet-like nanostructures of CoS. As shown in Figure 1(d and e), a similar morphology was seen, when the volume ratio of En to water (9:1) was used and named as CoS/En-snanoflowers. This is due to the fact that the structure directing roles of organic amine influences on the formation and geometry of layered superstructures (Ma et al., 2017). The photo-picture of real peony flower is shown in Figure 1(f).

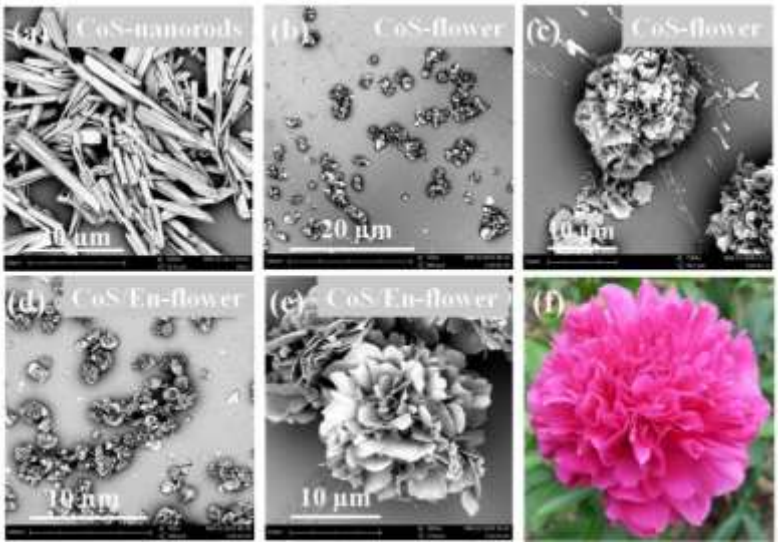


**Figure 1** SEM images of (a) CoS-nanorods, (b,c) peony flower-like CoS, (d,e) peony flower-like CoS/En, and (f) photo picture of peony flower in nature

To validate the crystal structure of CoS samples, XRD analyses were performed. As shown in Figure 2(a, curve i), the diffraction peaks at 2θ=30.4˚, 35.1˚, 46.6˚, and 54.2˚ in the XRD patterns correspond to respective (100), (101), (102) and (110) planes of CoS and matched well with the standard hexagonal CoS (space group of P63/mmc(194) (JCPDS no-75-0605). No other peaks from other phases were detected, implying high purity and single-phase crystallization of the product and no attached organic amine in the crystal structure of CoS nanorods. The XRD patterns of CoS-nanoflowers fabricated with $V_{En}$:$V_{H2O}$-1:9 are similar with that of CoS-nanorods as illustrated in Figure 2(a, curve ii). This is due to the fact that a small amount of En affects the morphology rather than crystal structure. Compared with the crystal structure of CoS-nanorods and CoS-nanoflowers, crystal structure of CoS/En-nanoflowers was different. The corresponding XRD patterns displayed in Figure 2(a, curve iii) stated that CoS–En inorganic–organic hybrid was mainly composed of amphorous CoS, considering the covalent organic-inorganic hybrid materials-based CoS layers coordinated through the bonding of the nitrogen atoms of ethylenediamine (En) (Gordillo et al., 2012).

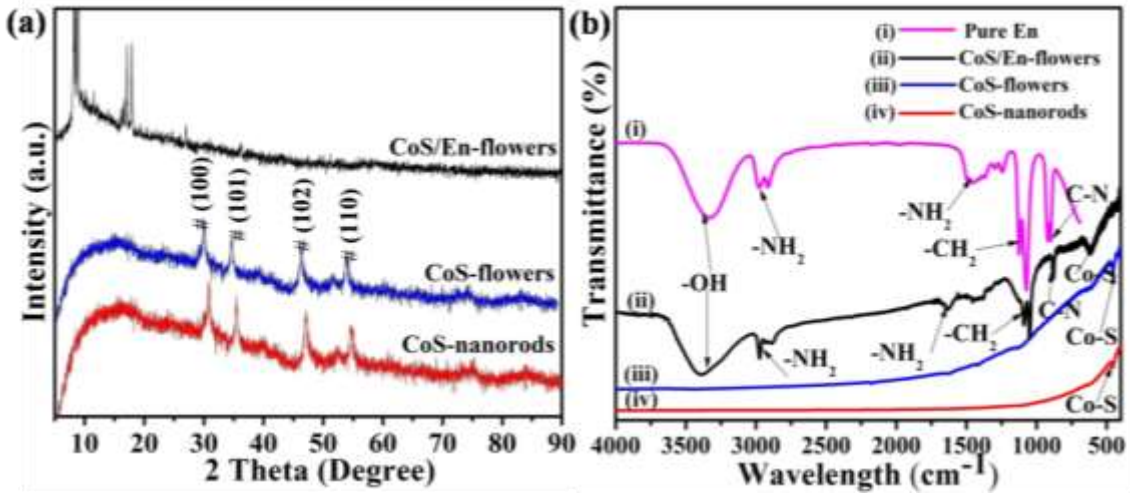


**Figure 2** (a) XRD patterns and (b) FT-IR spectrum of CoS samples including CoS/En nanoflowers, CoS-nanoflowers and CoS-nanorods

In order to attest the above statement, FT-IR spectroscopic measurements were carried out to confirm the preferential binding of the amine ligands to cationic sites on the surface of nanocrystals at growth stage as seen in Figure 2(b). The pure ethylenediamine (En) in pure liquid state is the *trans*-conformation structure which represented as broad and strong vibration bands in FT-IR spectra as shown in Figure 2(b, curve i). The standard spectrum of pure En shows characteristic bands corresponding to broad N–H deformation and stretching vibration at 3088 $cm^{-1}$ and 1612 $cm^{-1}$. $–CH_2–$ deformation vibration was visible at 1280–1520 $cm^{-1}$, and 1065 $cm^{-1}$ was assigned to C–N stretching (Hunyaid et al., 2017). As shown in Figure 2(b, curve ii), because of the chemical bonding between $Co^{2+}$ and the N atom of En, the stretching vibration band of the N–H shifted to the frequency around 2967 $cm^{-1}$ indicating that the amine groups of En is grafted on the inorganic crystal (Kang et al., 2017). Moreover, the new peak represented for Co–S stretching vibration appeared at 616 $cm^{-1}$ which was indicative of the CoS/En formation. In FT-IR spectrum of CoS-nanoflowers, the absence of vibration bands of N–H represented that there was no amine group of En attached with CoS sample as displayed in Figure 2(b, curve iii). Additionally, the band at 582 $cm^{-1}$ was attributed to Co–S stretching vibration in CoS phase. In CoS-nanoflowers formation, a small amount of En couldn't have the strong tendency of En binding in CoS crystal and En molecule could easily dissolve out in the reaction medium resulting in the pure CoS crystal. Considering a similar morphology, using a large amount of En was the decisive factor to give the amine functionalized CoS sample. In Figure 2(b, curve iv), almost all of the distinct peaks of En molecules haven't been seen in CoS-nanorods when water was used as solvent medium indicating that high purity CoS were obtained. Therefore, based on the above discussion of XRD and FT-IR analyses, the complete phase transformation occurred during the one-pot solvothermal/ hydrothermal route.

Considering the SEM images of Figure 1, the XRD patterns and FT-IR spectra of Figure 2, the sequential formation mechanism of peony flower-like CoS/En nanosheets could be proposed. It is well known that ethylenediamine (En) is a strong tridentate amine ligand with two $–CH_2$ groups to form chelates with metal ions in aqueous solutions. From the point of crystal formation mechanism, an ethylenediamine (En) molecule having a pair of binding sites for a $Co^{2+}$ ion produced a chemically stable complex $[Co(En)_x]^{2+}$ as written in Equation (6). Thiourea, sulfur precursor, acts as the reducing agent and reacted with water to form a sulfide ion ($S^{2–}$) as described in Equation (7) and (8). The reduced sulfide ion would react with $[Co(En)_x]^{2+}$ to form CoS/En as shown in Equation (9). Therefore, organic amine template-assisted fabrication was prominent to design nonlayered 2D atomically thin layer building blocks into 3D hierarchical structures through self-assembling growth process.

$$Co(CH_3COO)_2 + m\ (En \longrightarrow Co(En)_m(CH_3COO)_2 \quad (4)$$

$$H_2N–S–NH_2 \xrightarrow{\triangle} H_2S + HN=C=NH \quad (5)$$

$$H_2S \xrightarrow{\triangle} S^{2–} + H_2 \quad (6)$$

$$Co(En)_m(CH_3COO)_2 + S^{2–} \longrightarrow CoS(En)_m + 2(CH_3COO)^{–} \quad (7)$$

After a deep insight into a variety of CoS nanoadsorbents formation, the adsorption test was carried out by using different CoS samples. The adsorption efficiency toward Cr(VI) was evaluated at pH 5 through monitoring UV-Vis absorption spectra as shown in Figure 3(a). It is obvious that both CoS-nanorods and CoS-flowers gave less adsorption performance towards Cr(VI), with the removal efficiency of 30.8 mg/g and 64.3 mg/g, respectively. However, the obtained adsorption performance of Cr (VI) over CoS/En-nanoflowers exhibited much higher activity than that of its counterparts. Its adsorption efficiency of Cr(VI) reached to 87.7 mg/g within 40 min. A relatively high adsorption was obtained using CoS/En-nanoflowers as compared to those of CoS-nanorods

and CoS-nanoflowers that might be due to the morphological influence and activation of amine groups on adsorbent surface. Figure 3(b) represents the time-dependent UV-Vis absorption spectra of CoS/En-nanoflowers toward Cr(VI) concentration. With the increase in adsorption time, the absorption peak at 350 nm assigned to the Cr(VI) ions decreased gradually which demonstrated the adsorption capacity of Cr(VI) ions over CoS/En-nanoflowers at pH 5.

The time dependent adsorption rate is crucial factor for practical application. In order to better explore the adsorption kinetics of Cr(VI) ions, two kinetic models including pseudo-first-order (Eq- 4) and pseudo-second-order (Eq-5) were established and fitted with the experimental adsorption performance data of CoS/En-nanoflowers. The kinetic behavior of the adsorption process was studied at pH 5. The kinetic data were shown to be 0.071 $min^{-1}$ and 0.00130 g $mg^{-1}$ $min^{-1}$, respectively. The pseudo-second-order kinetic model showed the best correlated coefficient value ($R^2 > 0.995$) as compared with that of pseudo-first-order ($R^2 > 0.935$).

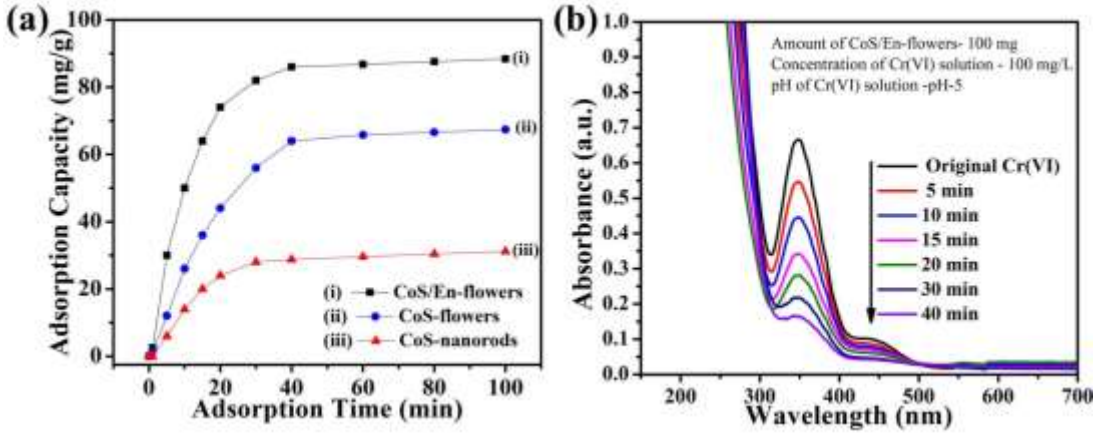


**Figure 3** (a) Cr(VI) adsorption performances on (i) CoS/En-nanoflowers, (ii) CoS-nanoflowers, (iii) CoS-nanorods at pH 5, (b) time dependent UV-Vis absorption spectra of Cr(VI) adsorption over CoS/En-nanoflowers at pH 5

The effect of pH strongly influences on the removal efficiency of Cr(VI) over adsorbents. The major Cr(VI) species exists mainly as $Cr_2O_7^{2-}$ and $HCrO_4^-$ in low pH solution, and were mainly in the form of $CrO_4^{2-}$ in natural aqueous solution. The variation of solution pH may not only cause the change in protonation degree of the amine groups grafted on the CoS surface but also can change the forms of Cr(VI) ions in water (Pakade et al., 2019). The experiments on the effect of pH on the Cr(VI) adsorption over CoS/En-nanoflowers were conducted. The removal of Cr(VI) ions decreased with increase in pH. It can be found that the maximum adsorption capacity was 90.8 mg/g and 87.7 mg/g in pH 2 and pH 5 aqueous solutions within 40 min. Conversely, at pH 8, much lower amounts of Cr(VI) (58.30 mg/g) were adsorbed on the CoS/En-nanoflowers under similar experimental conditions. The above investigations on the adsorption performance of CoS/En-nanoflowers found that the electrostatic interaction played a vital role in capturing negatively charged Cr(VI). To prove the interaction between the CoS/En-nanoflowers and the Cr(VI), the Zeta potential measurements over CoS/En-nanoflowers before and after adsorption were performed at different pHs. The surface charges of CoS/En-nanoflowers were revealed by Zeta potential as tabulated in Table (1). It can be seen that the surface of CoS/En-nanoflowers had positive charges when pH was less than 6 that was due to the fact that amine group ($–NH_2$) created more active sites on the CoS surface for $H^+$ ions of the solution at low pH. So, the coverage of $H^+$ ions tended to give the positive charge surface of amine grafted CoS showing the positive values of +8.8 mV and +6.5 mV at pH 2 and 5 before adsorption. The increased positive charges on the surface were conducive to the adsorption of negatively charged Cr(VI) at low pH. The negatively charged Cr(VI) ions covered on the surface of CoS/En-nanoflowers showing the changes in surface charges after adsorption. Therefore, the surface charge of CoS/En-nanoflowers was distinctly

changed to negative charges (–13.2 mV and –10.8 mV) at pH 2 and 5 after adsorption performances. This was attributed to the fact that, the electrostatic attraction between the Cr(VI) (e.g., $Cr_2O_7^{2-}$ and $HCrO_4^-$) and the amine functionalized CoS/En nanoflowers was taken, resulting in a dramatic enhancement of the adsorption capacity. However, at pH 8, the potential of CoS/En-nanoflowers reached the negative value of –16.8 mV and –18.5 mV before and after adsorption. The concentration of $^-OH$ ions in the alkali solution had a tendency to repulse $–NH_2$ group of the amine grafted CoS surface resulting in more negative charges. There was the repulsion force between the negatively charged surface of CoS/En-nanoflowers and the Cr(VI) (e.g., $CrO_4^{-2}$) at pH 8 showing less amount of Cr(VI) adsorption.

**Table (1)** Zeta Potential of CoS/En-Nanoflowers at Different pH Values Before and After Adsorption

| pH | Surface Charge (mV) | |
|---|---|---|
| | Before Adsorption | After Adsorption |
| 2 | +8.8 | –13.2 |
| 5 | +6.5 | –10.8 |
| 8 | –16.8 | –18.5 |

Above observation revealed that the adsorption of Cr(VI) over CoS/En-nanoflowers was obviously described as the electrostatic attraction between the positive charge amine groups on the surface of adsorbent and the negative charge Cr(VI). On the other hand, according to the theory of hard and soft acid-base (HSAB), Cr (VI) is a hard acid and easy to form a stable complex with a hard alkali like amine and the interaction between Cr(VI) and amine has a high complexation rate. So, CoS/En-nanoflowers exhibited a high adsorption toward Cr(VI). The synthesis route of CoS/En-nanoflowers and tentative adsorption mechanism of Cr(VI) on CoS/En-nanoflowers is illustrated in Figure 4.

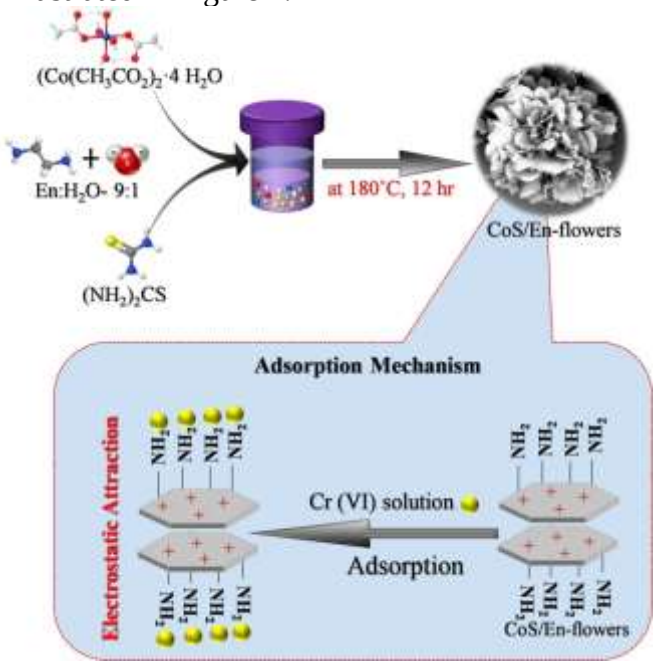


**Figure 4** Schematic illustration of processing steps of CoS/En-flowers adsorbent and mechanism of Cr(VI) ions adsorption on amine functionalized CoS surface

## Conclusion

In summary, inorganic-organic hybrid peony flower-like CoS nanosheets could be used as a nanoadsorbent for the removal of toxic Cr(VI) from aqueous liquid. CoS/En-nanoflowers exhibited a high adsorption efficiency and fast adsorption rate at pH 5 compared to that of its counterparts. The maximum adsorption capacity of the CoS/En-nanoflowers was found to be 87.7 mg/g within 40 min. Based on the zeta potential results at different pH, the adsorption mechanism investigation described that the main driving force for capturing Cr(VI) was the electrostatic interaction between the surface of adsorbent and Cr(VI).

## Acknowledgements

This work was supported by the National Natural Science Foundation of China (Grant Nos. 51173033, 51572060, 51502062) and Excellent Youth Foundation of Heilongjiang Scientific Committee (No. JC2015010).

## References

Gordillo, A. H., F. Tzompantzi, and R. Gomez, (2012) "Enhanced Photoreduction of Cr(VI) using ZnS(en)0.5 Hybrid Semiconductor" *Catalysis Communications*, Netherlands, vol. 19, pp.51-55.

Gupta, A., V. Sharma, K. Sharma, V. Kumar, S. Choudhary, P. Mankotia, B. Kumar, H. Mishra, A. Moulick, A. Ekielski, and P. K. Mishra, (2021) "A review of Adsorbents for Heavy Metal Decontamination: Growing Approach to Wastewater Treatment" *Materials (Basel)*, United Kingdom, vol. 14, pp.1-45.

Hunyaid, D., E. Majzik, J. Matyasi, J. Balla, A. Domjan, A. Szegedi, and I. M. Szilayi, (2017) "WO3–EDA Hybrid Nanoplates and Nanowires: Synthesis, Characterization, Formation Mechanism and Thermal Decomposition" *RSC Advance*, United Kingdom, vol. 7, pp.46726-46737.

Kang, H. J., and J. H. Kim, (2017) "Utilization of a ZnS(en)0.5 Photocatalyst Hybridized with a CdS Component for Solar Energy Conversion to Hydrogen" *Power Technology*, United Kingdom, vol. 28, pp. 2438-2444.

Liu, Y. W., H. Cheng, M. J. Lyu, S. J. Fan, Q. H. Liu, and W. H. Zhang, (2014) "Low Overpotential in Vacancy-Rich Ultrathin CoSe2 Nanosheets for Water Oxidation" *Journal of The American Chemical Society*, United States, vol. 136, pp.15670-15675.

Manyangadze, M., N. H. M. Chikuruwo, T. B. Narsaiah, C. S. Chakra, M. Radhakumari, and G. Danha, (2020) "Enhancing Adsorption Capacity of Nano-Adsorbents via Surface Modification: A Review" *South African Journal of Chemical Engineering*, Netherlands, vol 31, pp.25-32.

Ma, T., F. Zhou, T. W. Zhang, H. B. Yao, T. Y. Fu, Z. L. Yu, L. L. Li, and S. H. Yu, (2017) "Large-Scale Syntheses of Zinc. Sulfide. (Diethylenetriamine)0.5 Hybrids as Precursor for Sulfur Nanocomposites Cathodes" *Angewandte Chemie International Edition*, United Kingdom, vol 56, pp.11836-11840.

Pakade, V. E., N. T. Tavengwa, and L. M. Madikizela, (2019) "Recent Advances in Hexavalent Chromium Removal from Aqueous Solutions by Adsorptive Methods" *RSC Advances*, United Kingdom, vol. 9, pp. 26142–26164

Wu, X., R. Xu, R. J. Zhu, R. Wu, and B. Zhang, (2015) "Converting 2D Inorganic-Organic ZnSe-DETA Hybrid Nanosheets into 3D Hierarchical Nanosheets based ZnSe Microspheres with Enhanced Visible-Light-Driven Photocatalytic Performances" *Nanoscale*, United Kingdom, vol. 7, pp. 9752-9759.

Yein, W. T., Q. Wang, J. Z. Wu, X. H. Wu, (2018) "Converting CoS-TEA Hybrid Compound to CoS Defective Ultrathin Nanosheets and Their Enhanced Photocatalytic Property" *Journal of Molecular Liquids*, Netherlands, vol. 268, pp. 273-283.